Journal of Alloys and Compounds 509 (2011) 1040–1044

Contents lists available at ScienceDirect

Journal of Alloys and Compounds

journal homepage: www.elsevier.com/locate/jallcom

Morphology control and electrochemical properties of nanosize $LiFePO_4$ cathode material synthesized by co-precipitation combined with in situ polymerization

Ying Wang [a,*], Bing Sun [a], Jinsoo Park [b], Woo-Seong Kim [c], Hyun-Soo Kim [d], Guoxiu Wang [a,*]

[a] Department of Chemistry and Forensic Science, University of Technology, Sydney, City Campus, Broadway, Sydney, NSW 2007, Australia
[b] WCU Center for Next Generation Battery, Gyeongsang National University, 900 Gazwa-dong, Jinju 600-701, Republic of Korea
[c] Daejung Energy Materials Co., Ltd., Namdong-gu, Incheon 405-820, Republic of Korea
[d] Battery Research Center, Korean Electrotechnology Research Institute, Changwon 641-120, Republic of Korea

ARTICLE INFO

Article history:
Received 29 July 2010
Received in revised form 16 August 2010
Accepted 27 August 2010
Available online 20 October 2010

Keywords:
Co-precipitation
Polymerization
Carbon layer
$LiFePO_4$
Electrochemical properties

ABSTRACT

Nanosize carbon coated $LiFePO_4$ cathode material was synthesized by in situ polymerization. The as-prepared $LiFePO_4$ cathode material was systematically characterized by X-ray diffraction, thermogravimetric–differential scanning calorimetry, X-ray photo-electron spectroscopy, field-emission scanning electron microscopy, and transmission electron microscopy techniques. Field-emission scanning electron microscopy (FESEM) and transmission electron microscopy (TEM) images revealed that the morphology of the $LiFePO_4$ consists of primary particles (40–50 nm) and agglomerated secondary particles (100–110 nm). Each particle is evenly coated with an amorphous carbon layer, which has a thickness around 3–5 nm. The electrochemical properties were examined by cyclic voltammetry and charge–discharge testing. The as-prepared $LiFePO_4$ can deliver an initial discharge capacity of 145 mAh/g, 150 mAh/g, and 134 mAh/g at 0.2 C, 1 C, and 2 C rates, respectively, and exhibits excellent cycling stability. At a higher *C*-rate (5 C) a slight capacity loss could be found. However after being charge–discharge at lower *C*-rates, $LiFePO_4$ can be regenerated and deliver the discharge capacity of 145 mAh/g at 0.2 C.

1. Introduction

Since Padhi et al. did their breakthrough work on phospho-olivine polyanionic compound in 1997 [1], lithium iron phosphate ($LiFePO_4$) has become one of the most promising cathode materials for lithium ion batteries. Lithium iron phosphate exhibits several outstanding properties in terms of better cycling stability [2], superior thermal stability [3], low cost, and environmental friendliness [4]. Consequently, in electrical and hybrid electrical vehicles (EVs/HEVs), backup power systems, and other energy storage devices, $LiFePO_4$ has fulfilled most of the principal requirements, i.e. non-toxicity, low cost, safety, higher power/energy density, and excellent rate capability and long cycle life [5]. However, lithium iron phosphate suffers two major disadvantages, such as low electronic conductivity ($\sim 10^{-9}$ S cm^{-1}) and a slow lithium ion diffusion coefficient ($\sim 1.8 \times 10^{-14}$ cm^2 s^{-1}) [6], resulting poor electrochemical performance, especially poor rate capability. Researchers have been committed to developing better solutions to optimize its properties in order to successfully utilize lithium iron phosphate as cathode material in lithium ion batteries for EVs/HEVs, or other high power applications. Among those techniques, cation doping [7–9], and coating or embedding with conductive layers, particularly from carbon [10,11], have stood out as reliable methods to improve its electronic conductivity. With regard to the carbon effects, more attention has been focused on how to perfect the carbon coating layer using different primary carbon sources and how to achieve the most efficient coating method, because this conductive layer absolutely plays an important role in improving conductivity and facilitating the delithiation and lithiation processes [3,12]. However, due to the fact that carbon, when contributed as part of the cathode materials, would decrease the theoretical capacity of cathode material, many researchers have tried to reduce the carbon content to reach higher energy density and tap density [13,14]. Doeff et al. [15] reported that the morphology and characteristic of residual carbon can affect the electrochemical performance of $LiFePO_4$, i.e., the higher the content of carbon sp^2 character in the coating, the better are the electrochemical properties that can be expected. Recently, there are many reports on the synthesis of $LiFePO_4$ by using polymeric additive (PA). The polymers used include polyaniline (PAn) [16], polypyrrole (PPy) [17], polyethylene [18], polyetheramine [19], and polystyrene [20]. These polymer additives not only possess electrochemical activity by itself, but also form a carbonaceous deposit on the surfaces of particles, to suppress the crystal growth and the content of impurity phase ($Li_3Fe_2(PO_4)_3$). Therefore, polymers have

* Corresponding authors. Tel.: +61 2 9514 1786; fax: +61 2 9514 1656.
E-mail addresses: iriswang53@gmail.com (Y. Wang), Guoxiu.Wang@uts.edu.au (G. Wang).

0925-8388/$ – see front matter © 2010 Elsevier B.V. All rights reserved.
doi:10.1016/j.jallcom.2010.08.161

become an ideal substitute for other carbon sources in the synthesis of $LiFePO_4$.

In addition, the low Li-ion diffusion rate can be overcome by particle size minimization [21,22]. Gaberscek et al. [23] have claimed that smaller particle size is a key factor that enhances the properties of $LiFePO_4$ because a shorter lithium ion transport length and lower electrode resistance can be achieved. Delacourt et al. [21] further demonstrated that carbon-free $LiFePO_4$ can deliver a capacity of 147 mAh/g at the 5 C-rate when the particle size is controlled to be around 140 nm. In this regard, several methods have been proposed to minimize the particle size of $LiFePO_4$, for instance, sintering at lower temperature [6], co-precipitation in an aqueous medium [24,25], hydrothermal synthesis [26], mechanical activation [22,27], and chemical vapor deposition [28].

Based on the previous research work, we believe the electrochemical performance of $LiFePO_4$ can be improved by forming a conductive layer, while simultaneously minimizing their particle size. In this paper, the co-precipitation method was chosen as the synthetic method for the precursor, because of the feasibility of controlling the morphology and the accessibility of cheap raw materials. At the same time, aniline monomer, a highly conductive polymer, has been chosen as the carbon source during polymerization. Nanocrystalline $LiFePO_4$ with carbon coating layer was prepared by a reduction process.

2. Experimental

2.1. Material synthesis

$FePO_4$/PAn composite was synthesized through a spontaneous precipitation and polymerization in an aqueous solution. Typically, stoichiometric $NH_4H_2PO_4$ (0.4671 g, 98.5%, Sigma–Aldrich), aniline monomer (200 μl, 99%, Sigma–Aldrich), and HCl (37%, Sigma–Aldrich, equimolar with aniline) were dissolved in 50 ml distilled water. Then, 50 ml aqueous solution of H_2O_2 (4 ml, 50 wt%, Sigma–Aldrich) and $FeSO_4{\cdot}7H_2O$ (1.1233 g, 99%, Sigma–Aldrich) were both added to the above-mentioned solution under vigorous stirring at room temperature, and a black precipitate emerged. After stirring for 5 h, the resultant precipitant was washed for 3 times with distilled water, filtered, and dried at 50 °C overnight in vacuum. To synthesize $LiFePO_4$, 0.1 mol $LiCH_3COO$ (100%, Sigma–Aldrich), 0.1 mol as-prepared $FePO_4$/PAn precursor, and 0.06 mol L-ascorbic acid (VC) (99%, Sigma–Aldrich) were dispersed in ethanol and ultrasonicated for 30 min. After stirring the suspension for 5 h at 60 °C, the alcohol-insoluble amorphous precipitate was separated by filtration, washed with distilled water, and dried at 50 °C overnight in vacuum. Finally, crystalline $LiFePO_4$ was obtained by sintering the amorphous $LiFePO_4$ at 350 °C for 5 h, and then at 650 °C for 15 h.

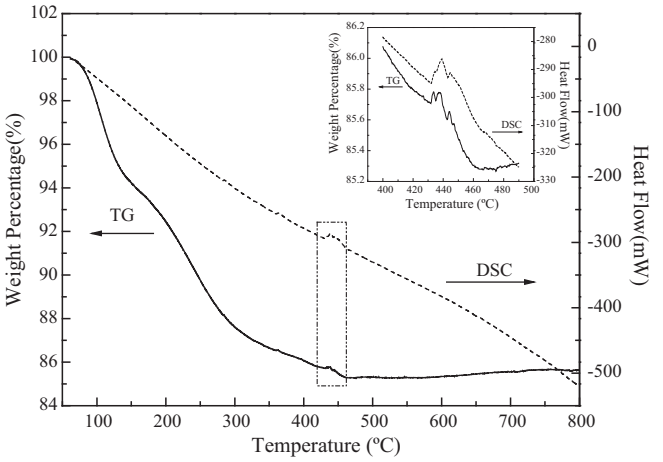

Fig. 2. TG-DSC curves of $LiFePO_4$ precursor measured at a heating rate of 5 °C/min in the Ar flow between RT and 800 °C with a zoom-in area as an insert.

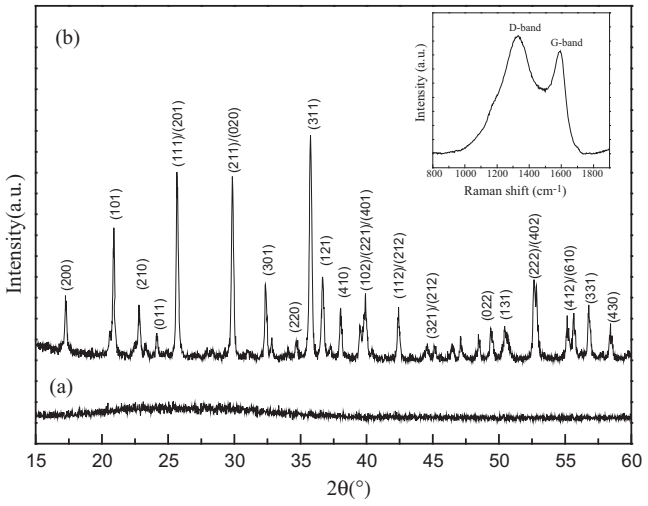

Fig. 3. XRD patterns of amorphous precursor (a), crystallized $LiFePO_4$ (b) and Raman spectrum of $LiFePO_4$ as an inset.

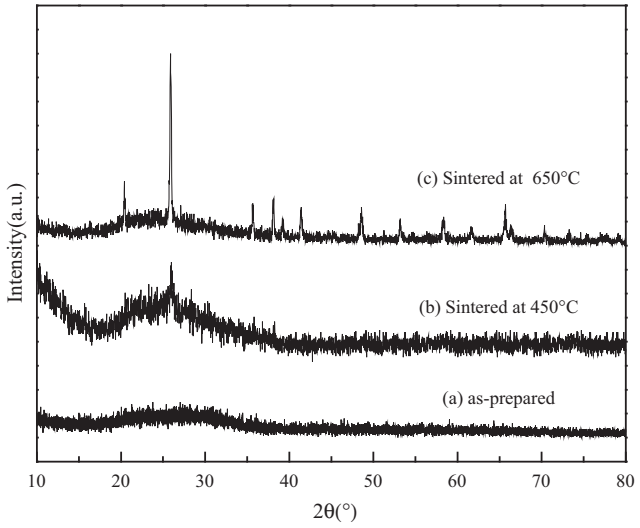

Fig. 1. XRD patterns of the amorphous $FePO_4$ and crystallized $FePO_4$ sintered at different temperature.

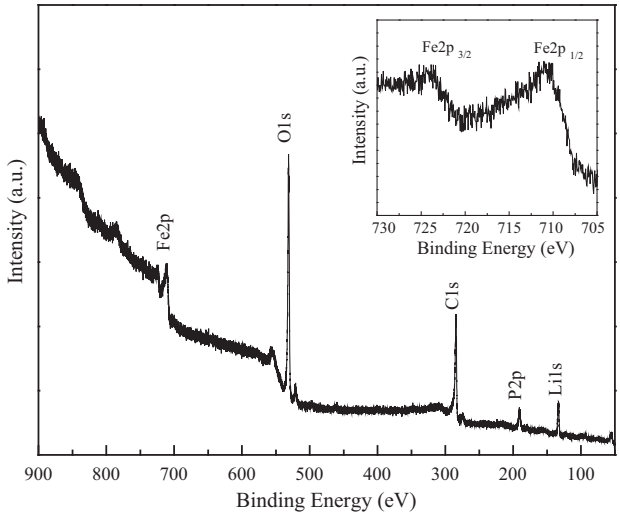

Fig. 4. XPS pattern of $LiFePO_4$ with a high-resolution XPS Fe2p spectrum as an insert.

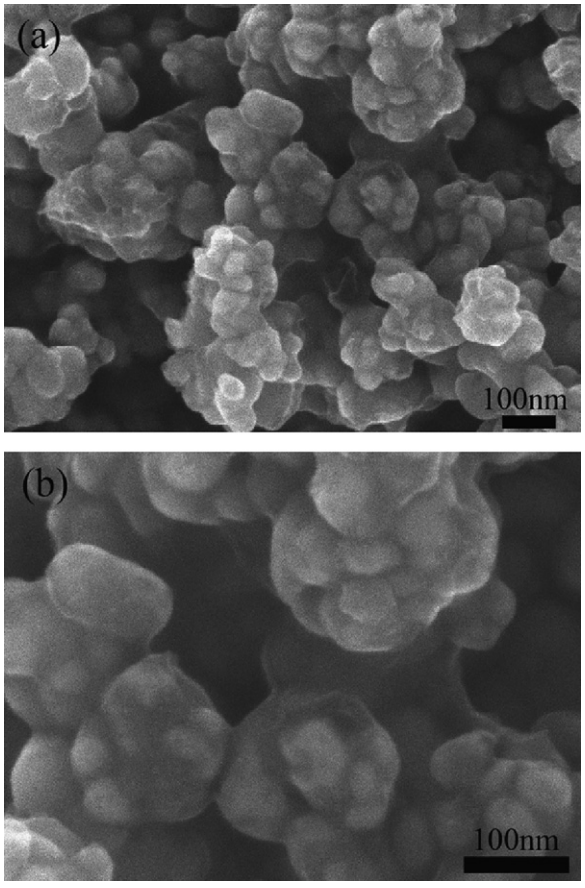

Fig. 5. FESEM images of $LiFePO_4$ after sintered at 650 °C for 15 h at different magnification.

2.2. Structural and physical characterization

Thermogravimetric–differential scanning calorimetry (TG–DSC) was conducted on a TGA/DSC1 thermogravimetric analyzer between 35 °C and 800 °C at a heating rate of 5 °C/min under argon atmosphere. X-ray diffraction (XRD) was conducted to determine the phase of the precursors and the as-prepared $LiFePO_4$ by using a GBC MMA X-ray diffractometer with Cu Kα radiation. Raman spectroscopy was performed with a Jobin Yvon HR800 confocal Raman system with a laser wavelength of 632.81 nm on a 300 lines/mm grating at room temperature. X-ray photoelectron spectroscopy (XPS, Axis Nova) was performed to confirm the oxidation state in the final product. The surface morphology and particle size distribution were observed using field-emission scanning electron microscopy (FESEM, JEOL7500) and transmission electron microscopy (TEM, JEOL JEM 2011).

2.3. Electrochemical characterization

The electrochemical characterization of $LiFePO_4$ was conducted on CR2032 coin cells, which were assembled in an argon-filled glove box (Mbraun, Unilab, Germany) using $LiFePO_4$ as the cathode material, lithium foil as the counter electrode, and 1 M $LiPF_6$ in a mixture of ethylene carbonate and dimethyl carbonate (EC:DMC = 1:1) as the electrolyte. After dispersing 80 wt% active material, 12 wt% carbon black, and 8 wt% polyvinylidene fluoride (PVDF) in n-methyl pyrrolidinone (NMP) to form a slurry, the cathode was made by spreading the slurry onto Al foil. After vacuum drying at 110 °C, the coated electrodes were pressed at 1200 kg/cm^2. Cyclic voltammetry (CV) was conducted on a CHI660B instrument in the voltage range of 2.5–4.2 V at different scan rates. The galvanostatic charge–discharge tests were performed at various current densities in the range of 2.0–4.2 V at room temperature.

3. Results and discussion

3.1. Structural analysis and surface characterization of the as-prepared $LiFePO_4$

The XRD patterns of the as-obtained $FePO_4$ are shown in Fig. 1. The diffraction line (a) indicates that the $FePO_4$ as initially prepared by the co-precipitation method is completely amorphous without any peaks. After heat-treating at 450 °C, one major broad peak at the 2θ of 25.9° can be detected in the diffraction line (b), which

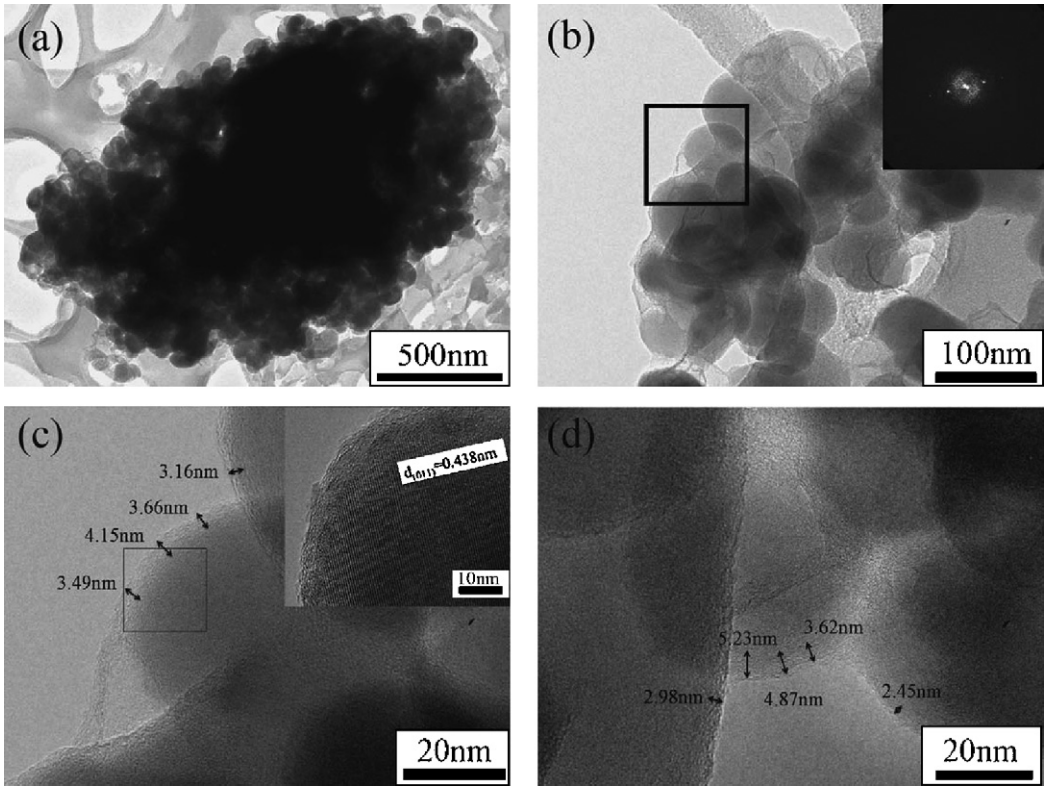

Fig. 6. TEM images of (a) $LiFePO_4$; (b) enlarged TEM image of spherical $LiFePO_4$ particles with a SAED as an inset; (c) zoom-in image of selected-area in (b) with enlarged *d*-spacing as an inset; (d) selected-area TEM image for $LiFePO_4$ containing several primary crystallites.

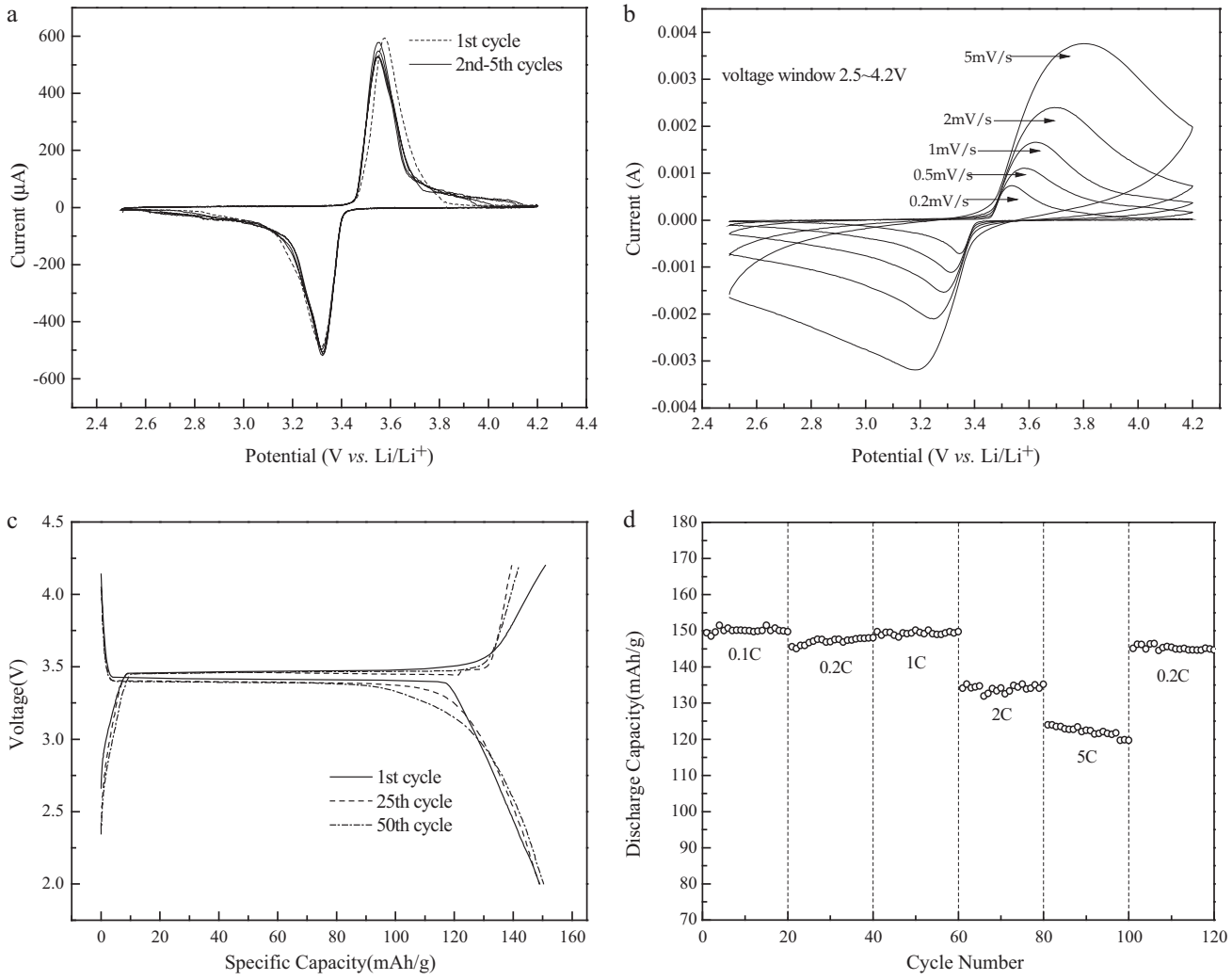

Fig. 7. Electrochemical properties of the as-prepared $LiFePO_4$ (a) cyclic voltammetry tests for the initial 5 cycles at the scan rate 0.1 mV/s in the potential window 2.5–4.2 V; (b) cyclic voltammetry tests at different scan rates in the potential window 2.5–4.2 V; (c) charge–discharge curves at different cycle number at 1 C-rate; (d) cycle capability at different discharge rates.

means that the precursor has begun to dehydrate, but still remains amorphous; while after sintering at 650 °C, as shown in the diffraction line (c), a series of diffraction peaks have emerged. The highest intensity peak, at the 2θ of 25.9°, can be assigned to anhydrous $FePO_4$ with a hexagonal structure (JCPDS card no. 29-0715) [4], indicating that amorphous $FePO_4$ has transformed into crystalline phase after heat treated at an elevated temperature.

The TG–DSC curves of $LiFePO_4$ precursor are displayed in Fig. 2 showing two obvious weight losses. The first weight loss occurred between room temperature and 150 °C, which is associated with the loss of physical absorption water in the as-prepared $LiFePO_4$. Following that, the second weight loss around 170–350 °C indicated the carbonization of polyaniline and might involve the decomposition of some residue organic chemicals. No appreciable weight loss can be found over the temperature range from 350 °C to 450 °C, but an exothermic peak is visible at 438 °C in the DSC curve, which is related to the crystallization of this compound.

Fig. 3 shows the XRD patterns of $LiFePO_4$ with a Raman spectrum as an inset. No peaks can be found in the diffraction line (a), which means the as-prepared $LiFePO_4$ has emerged in amorphous form. After sintering at 650 °C for 15 h, a series of sharp and symmetric diffraction peaks can be detected in the diffraction line (b), indicating that the $LiFePO_4$ is now highly crystallized and can be well indexed to ordered orthorhombic olivine structured $LiFePO_4$ (JCPDS card no. 40-1499, space group Pmnb (62)). The lattice parameters calculated by MDI. Jade.5.0 are $a = 5.985$ nm, $b = 10.306$ nm, $c = 4.681$ nm, and $V = 288.76\ nm^3$, which are quite close to the results of a previous report [24]. In addition, there is no diffraction peak of carbon in the final sample, in order to confirm the existence of the residual carbon, Raman spectroscopy was performed, as shown in the inset in Fig. 3. Two bands in the range of 1110–1480 cm^{-1} and 1480–1720 cm^{-1} are attributed to the D-band and G-band of carbon, respectively, which reveals that the carbon was amorphous.

X-ray photoelectron spectroscopy (XPS) measurement was conducted on the as-obtained $LiFePO_4$ to examine the oxidation state of Fe. As shown in Fig. 4, the binding energies (BE) of O1s, C1s, P2p, and Li1s were determined to be 531.2 eV, 284.4 eV, 133.4 eV, and 55.6 eV, respectively. Especially in the enlarged spectrum of Fe2p, shown as the inset in Fig. 4, one obvious peak and one satellite peak can be found at BEs of 710.9 eV and 723.8 eV, respectively, which correspond to Fe2p3/2 and Fe2p1/2 in $LiFePO_4$ [29]. Therefore, based on the XRD and XPS results, $LiFePO_4$ with high crystallinity and phase purity has been successfully synthesized.

3.2. FESEM and TEM observations of the as-prepared $LiFePO_4$

Fig. 5 shows the FESEM images of $LiFePO_4$. Ultra-fine primary particles with a size in the range of 40–50 nm have agglomerated to form larger secondary particles (with a size of about 100–110 nm). Fig. 5(b) clearly demonstrates that each secondary particle contains several primary particles and is wrapped in a thin layer of carbon. We believe that this layer was generated during the sintering process because of the carbonization of polyaniline. In order to further identify the structure of $LiFePO_4$, TEM observation was performed. Fig. 6(a) exhibits a large particle cluster with uniform agglomerated nanoparticles and Fig. 6(b) demonstrates that the typical particle size of $LiFePO_4$ is around 40–50 nm, with a continuous thin layer covering each particle, which is in agreement with the FESEM results. Selected-area electron diffraction (SAED), inset in Fig. 6(b), reveals that the as-prepared $LiFePO_4$ is highly crystalline. The enlarged image of selected area in Fig. 6(b) is shown in Fig. 6(c), the high-resolution TEM images have confirmed that each crystallite is spheroidal and completely coated by a carbon layer with a thickness ranging from 3 nm to 5 nm (indicated by arrows). Another zoom-in area in Fig. 6(d) also confirms the morphology of as-prepared $LiFePO_4$. Here, we emphasis that the conductive carbon layer is continuous, not only covering each primary crystallite, but also the outside of the agglomerated particles, so that it forms an efficient pathway for the lithiation and delithiation of lithium ions.

3.3. Electrochemical properties of the as-prepared $LiFePO_4$

In order to investigate the electrochemical properties of $LiFePO_4$, a series of electrochemical tests have been done. Fig. 7(a) shows the first 5 cycles of CV curves of $LiFePO_4$ composite in the voltage range of 2.5–4.2 V at the scan rate of 0.1 mV/s at room temperature. Negligible peak position shift can be found in the first oxidation peak compared with the subsequent four cycles, which indicates that $LiFePO_4$ has excellent coulombic efficiency and reversible capability. In Fig. 7(b) a series of redox peaks between 3.2 V and 3.8 V are assigned to $Fe^{2+/3+}$ at different scan rates. When the scan rate is increased gradually from 0.2 mV/s to 5 mV/s, the corresponding extraction and insertion of lithium ions can still be observed, which indicates superior rate performance of this material.

As shown in Fig. 7(c), $LiFePO_4$ can deliver 150 mAh/g initial discharge capacity with negligible capacity loss after 50 cycles at the 1 C between 2.0 V and 4.2 V. These curve present a long and flat voltage plateau, and exhibits excellent cycling stability with small voltage difference between charge and discharge process. The cycling capability of $LiFePO_4$ with increasing *C*-rates between 2.0 V and 4.2 V is presented in Fig. 7(d). The discharge capacity of $LiFePO_4$ is 149 mAh/g at 0.1 C. Furthermore, at higher *C*-rates (0.2 C, 1 C, 2 C and 5 C) the discharge capacity are 145 mAh/g, 150 mAh/g, 134 mAh/g and 127 mAh/g respectively, corresponding to a capacity retention of 97.3%, 100%, 90% and 85.2%, compared with the capacity at a rate of 0.1 C. The discharge capacity slightly deteriorate at the rate of 5 C as a function of cycle number, however, $LiFePO_4$ can be regenerated after being charge–discharged at lower *C*-rates again, and capacity retain back to 145 mAh/g at 0.2 C. This further confirms that by coating $LiFePO_4$ with a continuous conductive carbon layer through in situ polymerization, this ultra-fine $LiFePO_4$ composite can exhibit excellent electrochemical properties.

4. Conclusion

Nanosize $LiFePO_4$ was synthesized by co-precipitation combined with in situ polymerization. During the co-precipitation process, aniline monomers were polymerized and covered the surface of each newly formed $FePO_4$ particle, thus hindering the further growth of nuclei. Even though the $LiFePO_4$ was sintered at 650 °C for 15 h, the primary particle size of $LiFePO_4$ is still controlled within 40–50 nm, with a continuous carbon coating layer. The as-prepared $LiFePO_4$ can deliver an initial discharge capacity of 150 mAh/g at the rate of 1 C and exhibits excellent capacity retention and cycling stability at higher *C*-rates.

Acknowledgments

We thank the Australian Research Council for financial support through an ARC Linkage project (LP0989134), Bezel (Changzhou) New Energy Science & Technology Co., Ltd., and Daejung Energy Materials Co., Ltd. We also thank the assistance of Bei Wang for the Raman testing and Ivan Nevirkovets for the XPS measurement.

References

[1] A.K. Padhi, K.S. Nanjundaswamy, J.B. Goodenough, J. Electrochem. Soc. 144 (1997) 1188–1194.
[2] H. Huang, S.C. Yin, L.F. Nazar, Electrochem. Solid-State Lett. 4 (2001) A170–A172.
[3] H. Joachin, T.D. Kaun, K. Zaghib, et al., J. Electrochem. Soc. 156 (2009) A401–A406.
[4] P.P. Prosini, M. Carewska, S. Scaccia, et al., J. Electrochem. Soc. 149 (2002) A886–A890.
[5] Y. Wang, J. Wang, J. Yang, et al., Adv. Funct. Mater. 16 (2006) 2135–2140.
[6] L. Wang, G.C. Liang, X.Q. Ou, et al., J. Power Sources 189 (2009) 423–428.
[7] L. Wu, X.-h. Li, Z.-x. Wang, et al., J. Power Sources 189 (2009) 681–684.
[8] S.-h. Wu, M.-S. Chen, C.-J. Chien, et al., J. Power Sources 189 (2009) 440–444.
[9] M.R. Yang, W.H. Ke, J. Electrochem. Soc. 155 (2008) A729–A732.
[10] A.V. Murugan, T. Muraliganth, A. Manthiram, Electrochem. Commun. 10 (2008) 903–906.
[11] W. Xing-Long, J. Ling-Yan, C. Fei-Fei, et al., Adv. Mater. 21 (2009) 2710–2714.
[12] I. Belharouak, C. Johnson, K. Amine, Electrochem. Commun. 7 (2005) 983–988.
[13] Z.H. Chen, J.R. Dahn, J. Electrochem. Soc. 149 (2002) A1184–A1189.
[14] V. Pallomares, A. Goni, I.G. de Muro, et al., J. Electrochem. Soc. 156 (2009) A817–A821.
[15] M.M. Doeff, Y.Q. Hu, F. McLarnon, et al., Electrochem. Solid-State Lett. 6 (2003) A207–A209.
[16] L. Gangtie, Y. Xiaohua, W. Lei, et al., Polym. Adv. Technol. 20 (2009) 576–580.
[17] S.Y. Chen, B. Gao, L.H. Su, et al., J. Solid State Electrochem. 13 (2009) 1361–1366.
[18] A. Fedorkova, H.D. Wiemhofer, R. Orinakova, et al., J. Solid State Electrochem. 13 (2009) 1867–1872.
[19] C. Sisbandini, D. Brandell, T. Gustafsson, et al., J. Electrochem. Soc. 156 (2009) A720–A725.
[20] Y.H. Nien, J.R. Carey, J.S. Chen, J. Power Sources 193 (2009) 822–827.
[21] C. Delacourt, P. Poizot, S. Levasseur, et al., Electrochem. Solid-State Lett. 9 (2006) A352–A355.
[22] G.T.K. Fey, Y.G. Chen, H.M. Kao, 14th International Meeting on Lithium Batteries, Tianjin, Peoples R China, 2008.
[23] M. Gaberscek, R. Dominko, J. Jamnik, Electrochem. Commun. 9 (2007) 2778–2783.
[24] B.F. Wang, Y.L. Qiu, S.Y. Ni, Solid State Ionics 178 (2007) 843–847.
[25] J.C. Zheng, X.H. Li, Z.X. Wang, et al., Meeting of the International-Battery-Material-Association, Shenzhen, Peoples R China, 2007.
[26] Z.L. Wang, S.R. Su, C.Y. Yu, et al., Meeting of the International-Battery-Material-Association, Shenzhen, Peoples R China, 2007.
[27] M. Konarova, I. Taniguchi, J. Power Sources 194 (2009) 1029–1035.
[28] B. Zhao, Y. Jiang, H. Zhang, et al., J. Power Sources 189 (2009) 462–466.
[29] F. Yu, J.J. Zhang, Y.F. Yang, et al., J. Mater. Chem. 19 (2009) 9121–9125.